Journal of Physical and Theoretical Chemistry
of Islamic Azad University of Iran, 12 (2) 147-160: Summer 2015
(J. Phys. Theor. Chem. IAU Iran)
ISSN 1735-2126

Electronic, optical, thermodynamic parameter, NMR analysis on fullerene interacting with glycine by DFT methods

S. Dheivamalar and L. Sugi*

Department of Physics, Government Arts College for women, (autonomous) Pudukkottai, India

Received March 2015; Accepted June 2015

ABSTRACT

A series of exohedrally functionalized derivatives of D_3-symmetrical fullerene interaction with Glycine (NFG) have been investigated by using a DFT approach at the B3LYP/3-21G* basis sets. In the present investigation relative and formation energies of compounds, the highest occupied molecular orbital (HOMO) and the lowest unoccupied molecular orbital (LUMO), the Homo-Lumo band gap, chemical potential (μ), global softness(S), global electrophilicity index (ω), electro negativity (χ), hardness (η), were calculated for the title compound. In order to find the stable conformer, conformational analysis was performed based on Density Functional Theory B3LYP methods in 3-21G* basis set. The optical properties, thermodynamic properties and Mulliken charges of the NFG are calculated. A study of the electronic properties such as HOMO and LUMO energies, are performed by time – dependent DFT (TD-DFT) approach. The nuclear magnetic resonance (NMR) chemical shifts of the molecule is calculated by the gauge independent atomic orbital (GIAO) method. Moreover, their corresponding Homo-Lumo orbits are mainly associated with the surface of the cage. Surface modification and functionalization of nano-materials are very useful so that it could extend their applications in many fields especially metal ion adsorption, and catalytic process. It was concluded that it would be possible to produce novel specifically for bio-medical application.

Keywords: Fullerene; HOMO; LUMO; Thermochemistry; DFT

INTRODUCTION

The fullerenes have attracted great interest since they possess a large number of physical and chemical properties. A detailed report on the formation of organic derivatives on carbon clusters [1-7] has enhanced the stability of endohedral fullerenes [8-11]. This property leads to very interesting applications in medicinal chemistry, material science and nanotechnology [12]. There has been a steady increase in interest over a past few years in the interaction of biomolecules with carbon based nanostructures. Hu et al [13] have calculated energy and stability of glycine interacting with C_{60} compound. The theoretical investigation on C24 fullerene with various chemical groups also has been investigated [14]. To our knowledge, no theoretical reports have been found in the interaction of C_{12} fullerene with glycine. Several methods have been developed for the synthesis of

*Corresponding author: sugirdhamphy@gmail.com

fullerene amino acid derivatives. It was reported that glycine can directly react with fullerene through its amino group in the presence of sodium hydroxide [15-21]. Recently, it has been shown by using the hybrid density functional theory (B3LYP/3-21G*) calculations that fullerene cages might be unable to form stable bindings to proteins through their active sites. In this study, we examine the 'direct interaction of Glycine' with the walls of a (3,3) armchair carbon nanotube. Researchers think glycine may have a major role in cancer prevention because it seems to interfere with the blood supply needed by certain tumors. Because of this medicinal properties Glycine has been taken for the interaction with nanofullerenes.

The aim of the present work is to investigate the interaction of fullerene with glycine by using the hybrid DFT – B3LYP functional in conjugation with 3-21G* basis set. These interactions show the stability of the structure. Density Functional Theory is used for calculating the electronic structure, HOMO and LUMO energies, Mulliken charge of atoms, Molecular orbital analyses and NMR spectra of the title compound. These properties, increases the surface modification which is leading to the novel medical application. By investigating HOMO-LUMO energy gap the chemical stability against electronic excitation also have been studied. Thus, it would also possible to produce novel species for biomedical application; by attaching the carbon atom of glycine with the carbon atom of fullerene.

COMPUTATIONAL METHODS

In order to find the most stable structure, the optimization is done for nanofullerene with glycine, using B3LYP/3-21G* methods and basis set for various possible conformers. The computationally predicted various possible conformers are shown in Fig.1. The optimized molecular structure with the numbering of atoms of the title compound is shown in Fig. 2. The most optimized structural parameters were also calculated by B3LYP and have depicted in Table 1.All structures relating to structure of Glycine and nano fullerene Glycine (NFG) were designed primarily with the use of Gabedit 2.3.8 software; primary optimizations of structures were done with the use of the ground state method. For Glycine the C-C bond distance is around 1.5244 Å and the fullerene interacting with glycine in the C-C bond distance is around 1.544 Å.

RESULTS AND DISCUSSION

Global reactivity descriptors

The energies of frontier molecular orbital (ε_{HOMO}, ε_{LUMO}), energy band gap ($\varepsilon_{LUMO} - \varepsilon_{HOMO}$), electronegativity ($\chi$), chemical potential ($\mu$), global hardness ($\eta$), global softness ($S$), and global electrophilicity index (ω) [22–25] of nanofullerene interacting with glycine have been listed in Table 2. On the basis of ε_{HOMO} and ε_{LUMO}, these parameters are calculated using the equations (1) as given below

$$\mu = -\chi = \tfrac{1}{2}(\varepsilon_{LUMO} + \varepsilon_{HOMO})$$
$$\eta = \tfrac{1}{2}(\varepsilon_{LUMO} - \varepsilon_{HOMO}) \quad (1)$$
$$S = 1/2\eta$$
$$\omega = \mu^2/2\eta$$

Our calculation reveals that a large HOMO-LUMO gap of glycine molecule is 6.3506eV. The fullerene interacting with glycine has smaller HOMO-LUMO gaps than glycine, which indicates that the fullerene interacting with glycine is reactive. The glycine is found to be the most stable when compared with fullerene C_{12} interacting glycine (NFG).

Dipole moment, polarizability, hyperpolarizability, and thermodynamic properties

Dipole moment (μ), polarizability$\langle\alpha\rangle$, and total first static hyperpolarizabilities [26, 27] are also calculated by using density functional theory and shown in Table 3. The values can be expressed in terms of x, y, and $z$components and are given by following equations (2)

$$\mu = (\mu^2 x + \mu^2 y + \mu^2 z)^{1/2}$$
$$\langle\alpha\rangle = 1/3\ [\alpha xx + \alpha yy + \alpha zz] \quad (2)$$
$$\beta_{\text{Total}} = (\beta_x{}^2 + \beta y^2 + \beta z^2)^{1/2}$$

The βcomponents are reported in atomic units. Our calculations reveal that the dipole moment value of glycine is 1.2528 Debye. The dipole moment of Glycine is higher than the compound nanofullerene interacting with glycine and the value is 8.1190 Debye. We see a greater contribution of αzz in the molecule which shows that the molecule is elongated more towards Zdirection and is more contracted to Xdirection. Perpendicular part contributes with a less part of the polarizability of the molecule. βxxy and βxxx contribute with a larger part of hyperpolarizability in the molecule. This shows that XYplane and X-axis are more optically active in these directions. Standard thermodynamic functions such as free energy, constant volume heat capacity C_V, and entropy Shave also been calculated for Nano fullerene with glycine and the calculated values are given in Table 4.

Electronic spectra of fullerene c_{12} interacting with aminoacids

On the basis of fully optimized ground-state structure, DFT/B3LYP/3-21G* Calculations have been used to determine the low-lying excited states of fullerene. The theoretical results involving the vertical excitation energies, oscillator strength (f) and wavelength are carried out using the Gaussian 03 program. All molecules show strong π – π* and σ – σ* transition in the UV-Visible region with high extinction coefficients. The electronic spectra of glycine are shown in Fig.3a. In an attempt to understand the nature of electronic transitions in terms of their energies and oscillator strengths, time – dependent TD-DFT calculations involving configuration interaction between nanofullerenes with glycine (NFG) as shown in Fig.3b. Electronic transition determined from excited-state calculations are listed in Table 5 for the three lowest energy transitions of the molecule [28]. DFT calculations predict three intense electronic transition at 1.3051eV (949.99 nm), 1.6981 eV (730.15 nm) and 2.1699 eV (571.37 nm) with an oscillator strength of 0.0016, 0.0006, 0.0002 respectively.

Frontier molecular orbital analysis

Molecular orbital (HOMO & LUMO) and their properties such as energy are very useful for physicists and chemists and are very important parameters for quantum chemistry. The conjugated molecules are characterized by a small HOMO-LUMO separation, which is the result of a significant degree of intermolecular charge transfer from the end- capping electron – donor groups to the efficient electron – acceptor groups through π – conjugated path [29]. Both the HOMO-LUMOare main orbitals which take part in chemical stability [30]. The HOMO represents the ability to donate an electron, LUMO as an electron acceptor, represents the ability to obtain an electron.The HOMO and LUMO energy calculations by B3LYP/3-21G** method is shown the Fig. 4. This electronic absorption corresponds to the transition from the ground to the first excited state and is mainly described by one electron excitation from HOMO to LUMO orbital. While the energy of the HOMO is directly related to the ionization potential LUMO

energy is directly related to electron affinity. Energy difference between HOMO and LUMO orbital is called energy gapping which stability for structure [31]. Our calculation in order to evaluate the energy behavior of the title compound, the HOMO – LUMO energy gap was calculated at B3LYP/3-21G* level which reveals that the energy gap reflects the chemical activity of the molecule. The overlapping of

Orbital loops located on the HOMO and LUMO confirms the presence a resonance–assisted hydrogen bonding. The calculated energy value of HOMO is -9.3817eV and LUMO is -7.28781eV. The value of energy separation between the HOMO and LUMO is 2.09393eV explains the charge transfer interaction within the molecule, which influences the biological activity of the molecule.

Molecular orbital energy level diagram

In principle, there are several ways to calculate the excitation energies. The simplest one involves the difference between the highest occupied molecular orbital (HOMO) and the lowest unoccupied molecular orbital (LUMO) of a neutral system, and is a key parameter determining molecular properties. The frozen orbital approximation and the ground state properties are used to calculate the excitation values.

Our calculations reveal that the fullerene interacting with glycine has smaller HOMO-LUMO gaps than Glycine, which indicates that the NFG are reactive. The values of LUMO and HOMO and their energy gap reflect the chemical activity of the molecule. It should be noted that the LUMO energy levels of the NFG are comparable to the LUMO energy levels of glycine, and the HOMO energy levels of the NFG are close to the HOMO energy levels of glycine. The HOMO and LUMO distributions for the nanofullerene interacting with glycine (NFG) system are shown in Table 6. Large HOMO-LUMO gaps of glycine are associated with higher kinetic stability and low chemical reactivity, because it is not energetically favorable to add electrons to a high lying LUMO and to extract electrons from a low lying HOMO. From the chemical reactivity we can conclude that soft molecules will be more reactive than hard molecules.

Mulliken population analysis

Mulliken atomic charge calculation has an important role in the application of quantum chemical calculation of molecular system because of atomic charge effect dipole moment, molecular polarizability, electronic structure and more a lot of properties of molecular systems. The bonding capability of a molecule depends on the electronic charge on the chelating atoms. The atomic charge values were obtained by the Mulliken population analysis [32]. The calculated Mulliken charge values are listed in Table 7. The charge changes with basis set presumably occurs due to Polarization. The charge of N (15) atom is -0.459217e for B3LYP/ 3-21G* and - 0.809075e for B3LYP/ 3-21G** and the charge distribution of nitrogen atom is increasing trend in B3LYP/ 3-21G**. Considering all the methods and basis set used in the atomic charge calculation, the carbon atoms exhibit a substantial negative charge, which are donor atom. Hydrogen atom exhibits a positive charge, which is an acceptor atom. The C-N bond length of nanofullerene interacting with glycine is closer with normal C-N bond length (1.0052Å) due to the attraction effect between C-N atoms.

Interatomic bonded distance

In 1973, De Camp suggested that inter-atomic distancescan be used as chemical coordinates [33]. Only a brief description

of the methodology for the specific task of comparing structures is presented here. The algorithm begins by searching the target structure for a match for the first molecule in the molecular cluster. Molecules are matched by comparing atom types and atom connectivity using a modified graph-matching algorithm (Ullmann, 1976). Once a match has been found, the two structures can be superimposed to obtain a visual impression of their similarity. To obtain the best superposition, i.e. the best agreement between atomic positions, we use an algorithm for overlaying points (Kabsch, 1976, 1978). In which considers deviations between coordinates of atoms in the asymmetric unit. Molecules structures and is defined to obtain quantitative information on 1, 3- distances in X-M-Y linkages. We apply these principles to A…H-B hydrogen bond complexes. If a molecule match can be found, the search proceeds to search the target structure for a match for a molecule in the cluster. The only criterion used to choose this next molecule is that it be connected, through an interatomic distance constraint, to a molecule that has already been found [34].
In our present calculation all interatomic distances in the structure have specified convergence in molecule and as shown in the Table 8. The presence of a molecular cluster, the structure of which is described in terms of interatomic distances, within an infinite target. Structural based torsion angles around single bonds and large ranges of values due to thermal motions. The superimposed interatomic distance is used for weighing its distances to which standard dynamics. The atomic sites ncrease in dimensionality as the number of bond length increases within the molecules.

NMR spectral analysis

The isotropic chemical shifts are frequently used as an aid in identification of reactive organic as well as ionic species. It is recognized that accurate predictions of molecular geometries are essential for reliable calculations of magnetic properties. Therefore, full geometry optimization of NFG is performed by using B3LYP/3-21G* method. The range 13C NMR chemical shift of the typical organic molecule, usually is greater than 100 ppm the accuracy ensures reliable interpretation of spectroscopic parameters. In our present investigation, the chemical shift values of carbons are in the range 40.13 – 164.53 ppm. The oxygen has more electropositive property polarizes the electron distribution in its bond to adjacent carbon atoms and increases the chemical shift values. On the basis of 13C NMR spectra, in which the carbon (C4 and C18) atom has higher chemical shift 126.64 and 164.53 ppm than the other carbon atoms as shown in Table 9. Thus, first the same combination of method and basis set was used for the optimization and calculation of NMR properties. NMR computations (GIAO, NICS), a simple utility for obtaining tables of chemical shifts, averaged within specified groups of atoms can be used as shown in Fig.6. In the arrangement of molecules in a molecular cluster is captured using scalar interatomic distances drawn between neighboring molecules (dashed lines). For each pair of neighboring molecules in the cluster, we draw as many distances as there are atoms in the larger of the two molecules and bias the choice of distances towards the use of shorter rather than long distances as shown in Fig. 7.

Molecular electrostatic potential surface

Electrostatic potential (ESP) at a point in space around a molecule gives Information about the net electrostatic effect produced at that point by total charge distribution (electron+ proton) of the molecule and

correlates with dipole moments, electro negativity, partial charges and chemical reactivity of the molecules. It provides a visual method to understand the relative polarity of the molecule. An electron density is surface mapped with electrostatic potential surface depicts the size, shape, charge density and site of chemical reactivity of the molecules. This figure provides a visual representation of the chemically active sites and comparative reactivity of atoms [35].

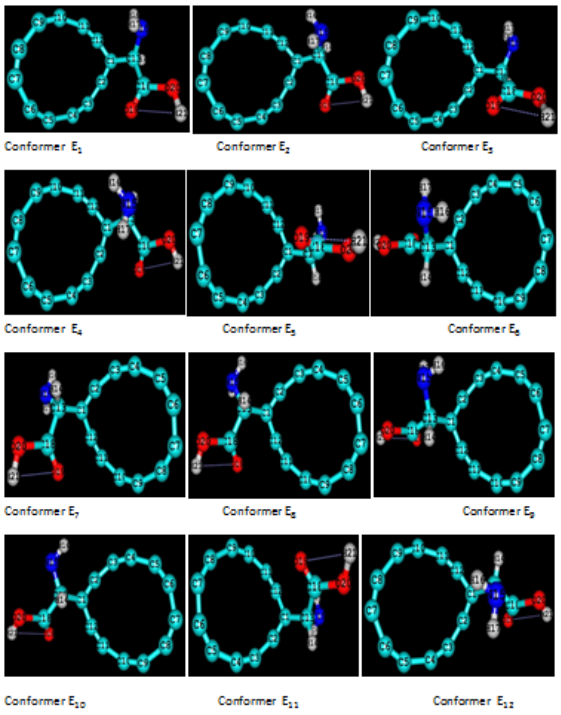

Fig. 1. Various possible conformers of nanofullerene with glycine.

Potential surface have been plotted for title molecule in B3LYP/3-21G* basis sets using the computer software Gauss view. In our present investigation the plots of the HOMO, LUMO and electrostatic potential are shown in Fig.8. The HOMO is found to be concentrated over the whole atoms, but the LUMO lies mainly over the molecules but less overlap. The electrostatic potential at the surface are represented by two different colors red represents regions of most electronegative, blue represents regions of the most positive electrostatic potential. Electrostatic potential maps are especially changes in reactive sites and to get an accurate indication of the absolute maximum charge transfer obtained for each molecule.

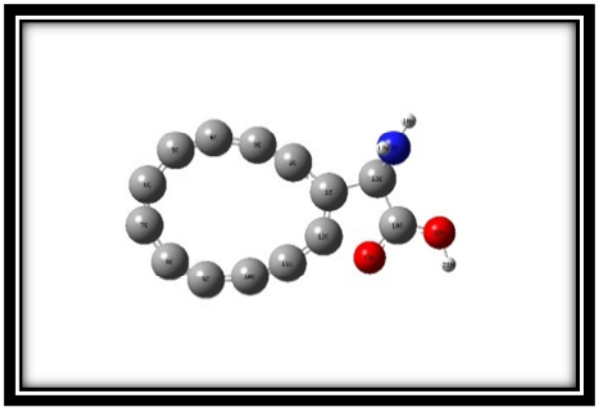

Fig. 2. Optimized structure of nanofullerene interacting with glycine.

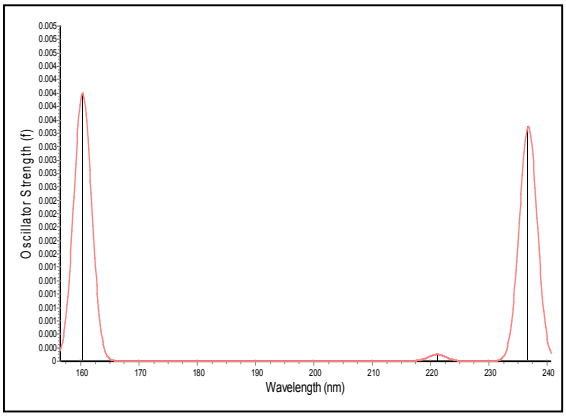

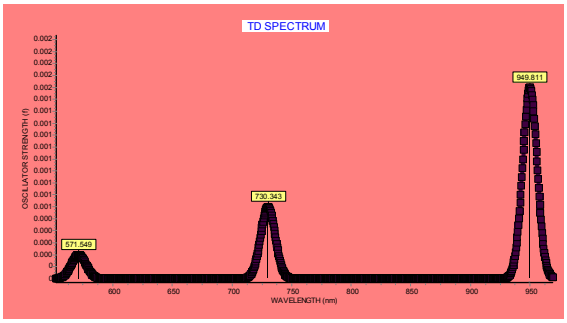

Fig. 3. UV – visible spectra of glycine (a) UV – visible spectra of nanofullerene with glycine (b).

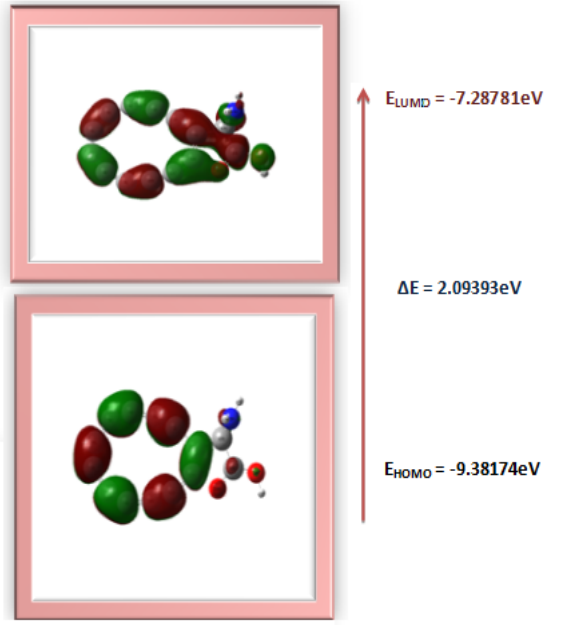

Fig. 4. HOMO-LUMO energy level diagram.

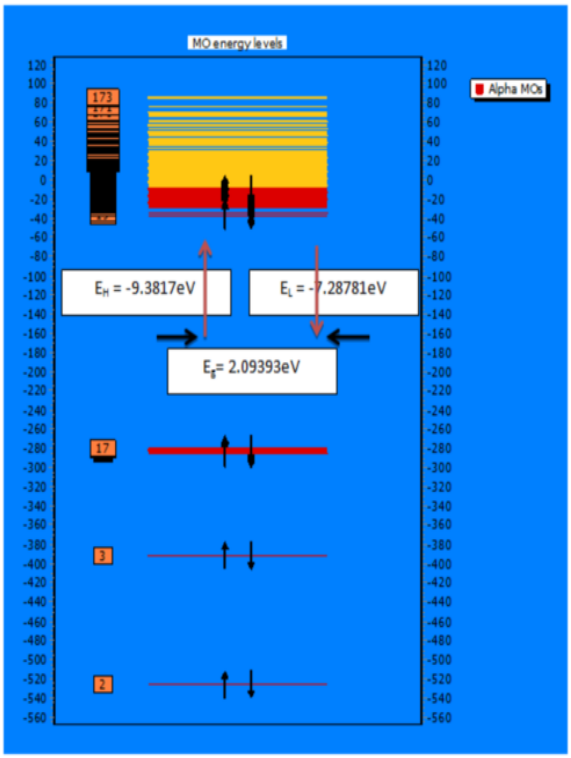

Fig. 5. Molecular orbital energy level diagram (highest occupied molecular orbital to lowest unoccupied molecular orbital.

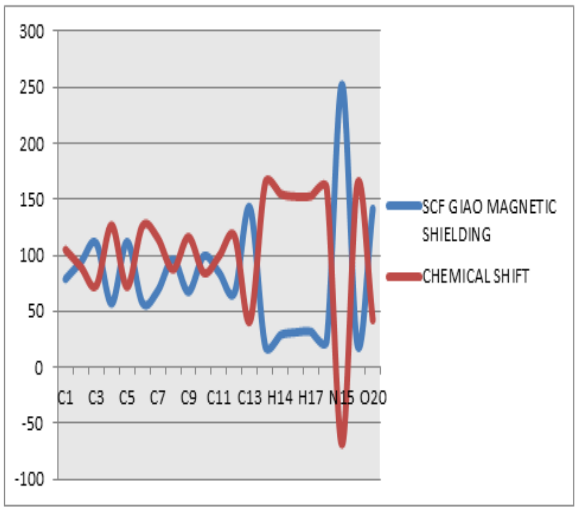

Fig. 6. NMR spectrum for combination of SCF GIAO magnetic shielding and chemical shift.

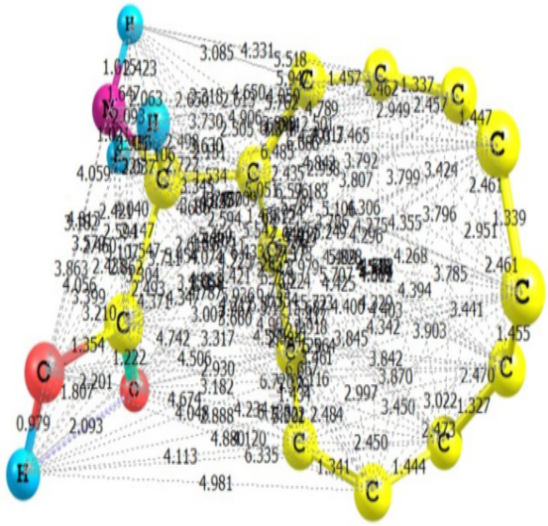

Fig. 7. The arrangement of molecules in a molecular cluster is captured using scalar interatomic distances drawn between neighbouring molecules (dashed lines). For each pair of neighbouring molecules in the cluster, we draw as many distances as there are atoms in the larger of the two molecules and bias the choice of distances towards the use of short rather than long distances.

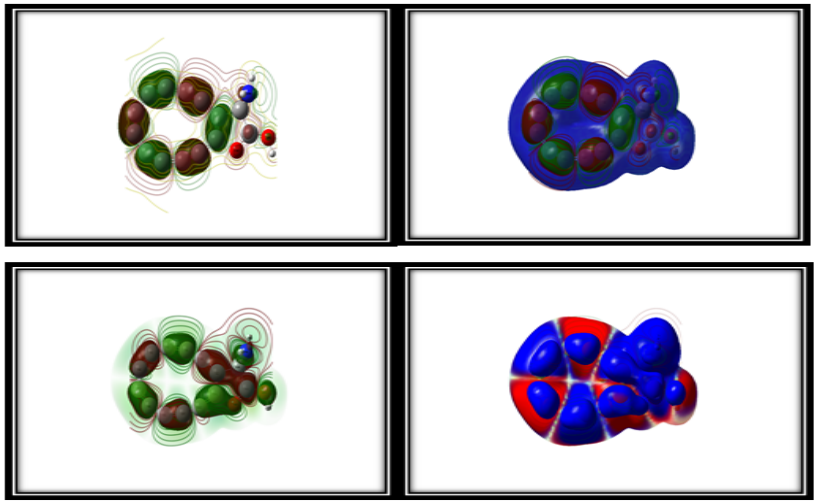

Fig. 8. Molecular electrostatic potential map of nanofullerene with glycine (NFG)**.**

Table 1. Optimized parameters of nanofullerene interacting with glycine, bond length (Å), and bond angle (°) by B3LYP/3-21G*

Optimized parameters	Bond length Å	Optimized parameters	Bond angle (°)
R (1,2)	1.4079	A (2,1,12)	122.24
R (1,12)	1.3518	A (2,1,13)	126.02
R (1,13)	1.544	A (12, 1, 13)	111.73
R (2,3)	1.2207	A (1,2,3)	167.19
R (3,4)	1.3567	A (2,3,4)	162.61
R (4,5)	1.2278	A (3,4,5)	152.99
R (5,6)	1.3577	A (4,5,6)	147.70
R (6,7)	1.2319	A (5,6,7)	144.84
R (7,8)	1.3574	A (6,7,8)	140.24
R (8,9)	1.2298	A (7,8,9)	151.83
R (9,10)	1.3525	A (8,9,10)	149.14
R (10,11)	1.2246	A (9,10,11)	165.03
R (11,12)	1.38	A (10,11,12)	162.53
R (12,19)	1.5457	A (1,2,11)	133.59
R (13,14)	1.0974	A (1,2,19)	107.51
R (13,15)	1.4313	A (11,12,19)	118.88
R (13,18)	1.5352	A (1,13,14)	108.37
R (15,16)	1.0038	A (1,13,15)	119.60
R (15,17)	1.0052	A (1,13,18)	98.94
R (18,19)	1.3025	A (14,13,15)	109.93
R (18,20)	1.2947	A (14,13,18)	105.93
R (20,21)	0.977	A (15,13,18)	112.86
		A (13,15,16)	116.95
		A (13,15,17)	117.22
		A (16,15,17)	115.27
		A (13,18,19)	114.43
		A (13,18,20)	123.70
		A (19,18,20)	121.84
		A (12,19,18)	107.30
		A (18,20,21)	115.50

Table 2. Calculated (εHOMO, εLUMO), energy band gap (εLUMO $-\varepsilon$HOMO), electronegativity (χ), chemical potential (μ), global hardness (η), global softness (S), and global electrophilicity index (ω)for the Nano Fullerene- Glycine by B3LYP/3-21G* levels of theory

MOLECULAR PROPERTIES	B3LYP / 3-21G*
EHOMO	-9.3817
ELUMO	-7.28781
Energy Gap	2.09393
Ionisation Potential (I)	9.3817
Electron affinity (A)	7.28781
Global Hardness (η)	1.046945
Chemical Potential (μ)	-8.334755
Global Electrophilicity (ω)	33.17657
Global Softness (S)	0.477580
Electronegativity (χ)	8.334755

Table 3. Calculated values of polarizability and hyperpolarizability using DFT/3-21G* for nano fullerene with glycine

POLARIZABILITY	VALUES	HYPERPOLARIZABILITY	VALUES
αxx	-30.2969	βxxx	168.45
αyy	-75.9781	βyyy	12.0870
αzz	-89.4817	βzzz	4.9901
αxy	-5.4188	βxyy	62.6475
αxz	-1.3424	βxxy	-46.0604
αyz	0.2765	βxxz	-3.3077
<α>	65.2522	βxzz	37.8960
-	-	βyzz	3.9989
-	-	βyyz	3.5181
-	-	βxyz	0.9766
		β_{Total}	270.7083

Table 4. Calculated thermodynamic properties of Nanofullerene with glycine by B3LYP/3-21G* methods

	E (Thermal) KCal/Mol	CV Cal/Mol-Kelvin	S Cal/Mol-Kelvin
Total	91.668	55.103	119.93
Translational	0.889	2.981	42.041
Rotational	0.889	2.981	32.898
Vibrational	89.890	49.141	44.995

Table 5. Calculated Parameters using TDDFT/B3LYP/3-21G* for Nano fullerene with glycine

Excitation	Expansion Wavelength (nm)	Oscillator Strength (f)	Energy (eV)
Excited State 1 55→56	949.99	0.0016	1.3051
Excited State 2 54→56 54→57	730.15	0.0006	1.6981
Excited State 3 55→57 55→58	571.37	0.0002	2.1699

Table 6. Molecular orbital energy level

1	-526.187715924	Occupied
2	-526.181457256	Occupied
3	-392.012214412	Occupied
4	-286.003984292	Occupied
5	-283.133160492	Occupied
6	-282.593010232	Occupied
7	-281.697748592	Occupied
8	-281.004124908	Occupied
9	-280.805752344	Occupied
10	-280.711872324	Occupied
11	-280.67268762	Occupied
12	-280.619897116	Occupied
13	-280.505608396	Occupied
14	-280.492274712	Occupied
15	-280.441661136	Occupied
27	-24.030836076	Occupied
28	-23.353811468	Occupied
29	-22.779374592	Occupied
30	-21.903433188	Occupied
51	-11.923306772	Occupied
52	-11.421252752	Occupied
53	-10.910763136	Occupied
54	-9.915634924	Occupied
55	-9.381743332	Occupied
	EHOMO = -9.38174eV ELUMO = -7.28781eV E = 2.093932eV	
56	-7.287810712	Unoccupied
57	-6.477449264	Unoccupied
58	-6.093493588	Unoccupied
59	-5.025438288	Unoccupied
60	-3.986227284	Unoccupied
171	77.025427076	Unoccupied
172	85.035161536	Unoccupied

Table 7. Calculated values of mulliken atomic charges

NANOFULLERENE INTERACTING WITH GLYCINE BY DFT			
B3LYP/3-21G*		B3LYP/3-21G**	
ATOM	CHARGES	ATOM	CHARGES
C1	-0.023776	C1	0.066248
C2	0.036893	C2	-0.077384
C3	-0.159544	C3	-0.268145
C4	0.030826	C4	0.043702
C5	0.080835	C5	0.111809
C6	0.094089	C6	0.112134
C7	0.083065	C7	0.143041
C8	0.093517	C8	0.096027
C9	0.057521	C9	0.111967
C10	-0.082922	C10	-0.220372
C11	-0.063866	C11	-0.180672
C12	0.328731	C12	0.581672
C13	-0.080565	C13	-0.105077
H14	0.272058	H14	0.357128
N15	-0.459217	N15	-0.809075
H16	0.242386	H16	0.380493
H17	0.230752	H17	0.373780
C18	0.844487	C18	1.135247
O19	-0.467049	O19	-0.670588
O20	-0.402277	O20	-0.681559
H21	0.344056	H21	0.499614

Table 8. Interatomic distances in molecules for nanofullerene with glycine

INTERATOMIC DISTANCES IN C12 WITH GLYCINE							
ATOM NUMBER	B3LYP/3-21G**	ATOM NUMBER	B3LYP/3-21G*	ATOM NUMBER	B3LYP/3-21G*	ATOM NUMBER	B3LYP/3-21G*
O20-H21	0.9770	C1-H17	2.7698	C3-H17	4.2467	O20-C10	5.9639
N15-H16	1.0038	O20-H14	2.8431	H17-H21	4.2995	O19-C4	5.9901
N15-H17	1.0052	C18-H17	2.9332	N15-C3	4.3034	C10-H21	6.0872
C13-H14	1.0974	H14-H17	2.9559	C4-C9	4.3196	C9-C13	6.0937
C2-C3	1.2207	O20-N15	2.9873	C11-H14	4.3344	C9-C18	6.1157
C10-C11	1.2246	O19-H14	2.9987	C12-H16	4.3420	O19-C8	6.1200
C4-C5	1.2278	C2-H14	3.0063	C4-C10	4.3533	O20-C3	6.1738
C8-C9	1.2298	C12-H14	3.0292	O19-H16	4.3553	C4-C18	6.2292
C6-C7	1.2319	C2-C11	3.0606	C3-C9	4.3983	C5-C13	6.2462
O20-C18	1.2948	C1-H16	3.2234	C4-C11	4.4269	C5-H14	6.5280
O19-C18	1.3025	N15-C2	3.2703	C5-C10	4.4526	C5-H17	6.5780
C9-C10	1.3521	C18-H16	3.2830	C3-C8	4.4536	C9-H14	6.5822
C7-C8	1.3573	C2-H17	3.3182	C2-C9	4.4569	C10-H16	6.7148
C11-C12	1.3800	C13-H21	3.3544	C4-C12	4.4961	O19-C5	6.7655
C1-C2	1.4079	C5-C8	3.3865	C2-C6	4.5785	N15-C5	6.7658
N15-C13	1.4312	C6-C9	3.3949	C7-C11	4.5374	C8-C13	6.8449
C13-C18	1.5352	C4-C7	3.4033	C3-H16	4.5484	C3-H21	6.8553
C1-C13	1.5440	C3-C12	3.4324	C1-C9	4.6232	C9-H17	6.8974

Table 8. Continued

019-C12	1.5456	O19-N15	3.4765	H16-H21	4.6232	O19-C7	6.9694
H16-H17	1.6973	O20-H17	3.4983	O20-C11	4.7486	C5-H16	7.0335
C18-H21	1.9289	C1-C10	3.5336	C8-C12	4.7749	C6-C13	7.0547
N15-H14	2.0792	N15-C12	3.5350	C10-C18	4.7980	N15-C9	7.0649
C13-H16	2.0878	O20-C12	3.5509	C11-H17	4.8182	C8-C18	7.0731
C13-H17	2.0919	C11-C18	3.5735	C2-C8	4.8329	O19-C6	7.1506
C18-C14	2.1177	C3-C6	3.5862	O19-C3	4.8380	C5-C18	7.1733
C1-H14	2.1574	C7-C10	3.5879	C5-C11	4.8454	C7-C13	7.2864
019-O20	2.2700	O20-C1	3.6032	N15-C11	4.8487	C8-H14	7.2909
H14-H16	2.2836	C8-C11	3.6049	C1-C5	4.8598	O20-C9	7.3034
C12-C18	2.2985	C2-C5	3.6207	C6-C11	4.9083	C6-H14	7.3893
O19-C1	2.3396	C12-H17	3.6333	C10-C13	4.9132	C9-H21	7.4393
C1-C18	2.3403	C2-H16	3.6526	C11-H21	4.9183	C6-H17	7.4776
O19-C13	2.3891	O20-H16	3.6649	C3-C18	4.9412	O20-C4	7.4839
C12-C13	2.3993	O19-C2	3.7007	C2-C7	4.9449	C8-H17	7.5265
O19-H21	2.4134	C2-C10	3.7071	O20-C2	4.9538	C7-H14	7.6757
C2-C12	2.4167	O19-H17	3.7099	O19-C9	5.0660	N15-C6	7.6980
C6-C8	2.4354	C3-C11	3.7124	C4-C13	5.1709	N15-C8	7.7318
C5-C7	2.4690	H14-H21	3.7170	C5-C12	5.2255	C6-C18	7.7685
N15-C18	2.4729	O19-C10	3.7171	C1-C8	5.3147	C9-H16	7.7766
C4-C6	2.4838	C2-C18	3.7232	C4-H14	5.4291	C7-H17	7.8272
C8-C10	2.4894	C11-C13	3.7667	C10-H14	5.4412	N15-C7	8.0535
O20-C13	2.4978	C3-C13	3.8212	C4-H17	5.4877	C6-H16	8.0818
C7-C9	2.5096	C9-C12	3.8481	C7-C12	5.5043	C4-H21	8.1231
C1-C11	2.5108	C4-C1	3.8894	C1-C6	5.5641	O20-C8	8.3071
C3-C5	2.5133	N15-H21	3.9001	C6-C12	5.6179	C8-H16	8.3576
O19-C11	2.5207	C12-H21	3.9013	N15-C4	5.6249	O20-C5	8.4539
C2-C4	2.5478	C4-C8	3.9962	C2-H21	5.6418	C8-H21	8.5218
C9-C11	2.5551	C3-C10	4.0080	C11-H10	5.6510	C7-H16	8.5582
N15-C1	2.5722	C5-C9	4.0382	C1-C7	5.7466	C5-H21	9.0189
C10-C12	2.5745	C3-H14	4.1037	C4-C16	5.8364	O20-C7	9.0450
C1-C3	2.6123	C6-C10	4.1942	C10-H17	5.8393	O20-C6	9.0614
C2-C13	2.6311	C3-C7	4.2444	N15-C10	5.9464	C7-H21	9.3764

Table 9. Calculated nmrscf giao magnetic shielding and chemical shifts (ppm) of nanofullerene with glycine by B3LYP/3-21G*

ATOM	SCF GIAO MAGNETIC SHIELDING	CHEMICAL SHIFT
C1	78.798	104.80
C2	93.964	89.63
C3	110.77	72.82
C4	56.95	126.64
C5	111.81	71.78
C6	57.64	125.95
C7	68.26	115.33
C8	96.30	87.29
C9	67.39	116.20
C10	99.29	84.30
C11	84.46	99.13

Table 9. Continued		
C12	66.66	116.93
C13	142.66	40.93
C18	19.06	164.53
H14	28.86	154.73
H16	31.26	152.33
H17	31.76	152.83
H21	23.57	160.02
N15	252.37	-68.77
O19	19.74	163.85
O20	141.35	42.24

CONCLUSIONS

A series of exohedrally functionalized derivatives of D_3-symmetrical fullerene have been investigated by using a DFT approach at the B3LYP/3-21G* basis sets. Relative and formation energies of compounds, the highest occupied molecular orbital (HOMO) and the lowest unoccupied molecular orbital (LUMO), the Homo-Lumo band gap, chemical potential (μ), global softness(S), global electrophilicity index (ω), electronegativity(χ), hardness(η), were calculated. On the basis of fully optimized ground- state structure, DFT/B3LYP/3-21G** Calculations have been used to determine the low-lying excited states of fullerene. It is also proved that fullerene ring might be unable to form stable binding to protein through their amino nitrogen, hydroxyl oxygen and carbonyl oxygen active sites. It was found that fullerene with glycine is most stable only through the active sites of carbon atom of fullerene interactions with the carbon atoms of glycine. The calculated value obtained from UV Spectra of Glycine before and after interaction with nanofullerene has been studied. The above studied shows nanofullerene interacting with glycine is higher dipole moment (8.1190 Debye) than glycine. The theoretical results involving the vertical excitation energies, oscillator strength (f) and wavelength are carried out. All interatomic distances in the structure and groups them by distance values with specified threshold convergence. All the methods and basis set used in the atomic charge calculation, the carbon atoms exhibit a substantial negative charge, which are donor atom. Hydrogen atom exhibits a positive charge, which is an acceptor atom. From the chemical reactivity we can conclude that soft molecules will be more reactive than hard molecules. This work can be useful for pharmaceutical researchers because this action causes interesting medicinal properties.

REFERENCES

[1]. M. Fanti, Z. Zrbetto, J.P. Galaup, J. Chem. Phys. 116 (2002) 7621.
[2]. E. Toth, R.D. Bolskar, A. Borel, J. Amer. Chem. Soc. 127 (2005) 799.
[3]. P.F. Coheur, J. lievin, R. Colin, B. J. Razbirib, Chem. Phys, 118 (2003) 550.
[4]. J.E. Riggs, Y.P. Sun, Ibid, 112 (2000) 4221.
[5]. B. Sitharaman, R.D. Bolskar, I. Rusakova, L.J. Wilson, Nano.Lett, 4 (2004) 2373.
[6]. R.H. Xie, G.W. Bryant, C.F. Cheung, J. Chem., Phys. 121 (2004) 2849.
[7]. X.J. Li, G.S. Jiao, J. Mol.Strucct. (Theochem). 893 (2009) 26.
[8]. Yu. N. Makurin, A.A. Sofronov, A.I. Gusev, chem., Phys, 270 (2001) 293.

[9]. T. Guo, R.E. Smalley, G.E. Scuseria, J. Chem. Phys. 99 (1993) 352.
[10]. M.H. Lin, Y.N. Chiu, S.T. Lai, J. Mol. Struct. (Theochem), 422 (1998) 57.
[11]. X.J. Li, Ibid. 896 (2009) 25-29 .
[12]. H. Prinzbach, A. Weiler, P. Landenberger, Nature 407 (2000) 60.
[13]. Y. H. Hu, E. Ruckenstein, Ibid, 850 (2008) 67.
[14]. S. Peng, X.J. li, Y. Zhang, S. Zhao. C. (2009)1095.
[15]. Y.Z. An, L.J. Rubin, J. Org. Chem. 58 (1993) 4788.
[16]. M. Prato, A. Bianco, M. Maggini, G. Scorrano, C. Toniolo, F. Wudl, J. Org. Chem. 58 (1993) 5578.
[17]. A. Kiebe, A. Hirsch, J. Chem. Soc., Chem. Commun. (1994) 335.
[18]. L. Isaacs, A. Wehrsig, F. Helv Diederich, Chim. Acta 76 (1993) 1231.
[19]. L. Isaacs, F. Diederich, Helv. Chim. Acta 76 (1993) 2454.
[20]. D.J. Zhou, L.B. Gan, L.B. Xu, C.P. Luo, C.H. Huang, Fullerene Sci. Technol. (1995) 3.
[21]. M.B. Messaouda, F. Moussa, B. Tangour, H. Szwarc, M. J. Abderrabba, Mol. Struct. Theochem 809 (2007) 153.
[22]. R. G. Pearson, Journal of Organic Chemistry, 54 (1989) 1423.
[23]. R. G. Parr, L. V. Szentp´aly, and S. Liu, 121 (1999) 1922.
[24]. P. K. Chattaraj and S. Giri, "Journal of Physical Chemistry A, 111 (2007) 11116.
[25]. J. Padmanabhan, R. Parthasarathi, V. Subramanian, and P. K. Chattaraj, Journal of Physical Chemistry A, 111 (2007) 1358–1361.
[26]. D. A. Kleinman, Physical Review B, 126 (1962) 1977.
[27]. J. Pipek and P. G.Mezey The Journal of Chemical Physics, 90 (1989) 4916.
[28]. S. A. Siddiqui, T. Rasheed, M. Faisal, A. Kumar Pandey, and S. Bahadar Khan, Spectroscopy: An International Journal, 27 (2012) 185.
[29]. S. Gunasekaran, R. ArunBalaji, S. kumaresan, G. Anand, S, Srinivasan, Can J Anal Sci Spectrosc, 53 (2008) 149.
[30]. D.F.V. Lewis, Ioannides C & Parke D V, Xenobiotica, 24 (1994) 401.
[31]. L. Padmaja, C. Ravikumar, D. Sajan, I.H. Joe, V.S. Jayakumar, G.R. Petti, O.F. Nielson, J Raman spectrosc, 40 (2009) 419.
[32]. R.S. Mulliken, J. Chem. Phys. 23 (1955) 1833–1840.
[33]. W.H. de Camp, Acta Crystallogr., Sect. A 29 (1973) 148.
[34]. V.P. Gupta, A. Sharma, V. Virdi, V.J. Ram, Spectrochim. Acta, 64 (2006) 57.